AGU PUBLICATIONS

Geophysical Research Letters

RESEARCH LETTER
10.1002/2017GL075044

Key Points:
- The ITCZ position and Hadley cell strengths are correlated with SSTs in the North Atlantic and North Pacific on multidecadal timescales
- Hemisphere mean tropospheric temperatures are more sensitive to North Atlantic than North Pacific SSTs
- Results suggest that heating and cooling of the extratropical atmosphere over the ocean connect the ITCZ position to North Atlantic SSTs

Supporting Information:
- Supporting Information S1

Correspondence to:
B. Green,
brianmg@mit.edu

Citation:
Green, B., J. Marshall, and A. Donohoe (2017), Twentieth century correlations between extratropical SST variability and ITCZ shifts, *Geophys. Res. Lett.*, *44*, doi:10.1002/2017GL075044.

Received 21 JUL 2017
Accepted 29 AUG 2017
Accepted article online 31 AUG 2017

Twentieth century correlations between extratropical SST variability and ITCZ shifts

Brian Green[1], **John Marshall**[1], **and Aaron Donohoe**[2]

[1]Department of Earth, Atmospheric, and Planetary Sciences, Massachusetts Institute of Technology, Cambridge, Massachusetts, USA, [2]Applied Physics Laboratory, University of Washington, Seattle, Washington, USA

Abstract The Intertropical Convergence Zone (ITCZ) is a global-scale band of tropical precipitation lying, in the annual mean, just north of the equator. Its position can be tied to the atmosphere's energy balance: the Northern Hemisphere is heated more strongly than the Southern Hemisphere, biasing the atmosphere's circulation and ITCZ north of the equator. In the context of this energy balance framework, we examine multidecadal connections between variations in the position of the global ITCZ and indices of extratropical sea surface temperature (SST) variability over the twentieth century. We find that the ITCZ and atmospheric circulation are shifted farther to the north during periods when North Atlantic and North Pacific SSTs are anomalously warm. Additionally, a warmer North Atlantic is correlated with a relatively warm Northern Hemisphere atmosphere. Our results suggest an important role for the ocean circulation in modulating ITCZ migrations on decade-and-longer timescales.

1. Extratropical Sea Surface Temperatures, Cross-Equatorial Energy Transport, and the ITCZ Position

The Intertropical Convergence Zone (ITCZ) occupies a narrow range of latitudes, particularly in the Atlantic and eastern Pacific oceans (Figure 1a). It is located between the atmosphere's two Hadley cells, which are responsible for the majority of the atmosphere's meridional energy transport in the tropics [cf. *Marshall et al.*, 2014, Figure 3], and migrates with those circulations over the course of the seasonal cycle [*Donohoe et al.*, 2013]. When the Sun heats the Northern Hemisphere (NH) atmosphere more strongly during boreal summer, the Hadley cells (and ITCZ) are centered north of the equator and transport energy southward across the equator, opposing the solar heating imbalance. The opposite occurs during boreal winter, when the Hadley cells and ITCZ are centered in the Southern Hemisphere (SH).

This relationship between interhemispheric heating contrasts and the position of the ITCZ can be found across a large range of timescales [e.g., *Donohoe et al.*, 2014; *McGee et al.*, 2014], and a framework has emerged for interpreting their connection [*Kang et al.*, 2009] (see the review in *Schneider et al.* [2014]). When the ocean, or a top-of-atmosphere radiative imbalance, preferentially heats one hemisphere's extratropical atmosphere relative to the other, eddies anomalously export a fraction of that energy into the tropics; the remainder is radiated away to space or stored in the climate system. The Hadley cells, and thus the ITCZ, shift into the warmer hemisphere and transport the excess energy across the equator into the cooler hemisphere. For example, northward cross-equatorial energy transport by the Atlantic meridional overturning circulation (AMOC), heating the NH and cooling the SH, has been argued by *Frierson et al.* [2013] and *Marshall et al.* [2014] to bias the ITCZ north of the equator in the annual mean. The sensitivity of the ITCZ position to interhemispheric heating contrasts has also been seen in climate models simulating a range of forcings, including changes in high-latitude ice cover [*Chiang and Bitz*, 2005], changes in the AMOC's energy transport [*Zhang and Delworth*, 2005; *Broccoli et al.*, 2006; *Sun et al.*, 2013], and global warming [*Frierson and Hwang*, 2012].

Across these simulations, changes in the sea surface temperature (SST) contrast between the NH and SH are correlated with meridional shifts in the Hadley cells and migrations of the ITCZ. Sea surface temperatures are only indirectly related to the heating or cooling of the atmosphere, but they have proven useful proxies when sufficient data to estimate the energy balance is unavailable [e.g., *Zhang et al.*, 2007]. Interhemispheric SST contrasts have been linked to ITCZ shifts in the paleoclimate record [*McGee et al.*, 2014], in model simulations of paleoclimate [*Donohoe et al.*, 2013], and appear to be connected to Sahel precipitation changes in the twentieth century (see the review in *Chiang and Friedman* [2012]). Here we take an observational

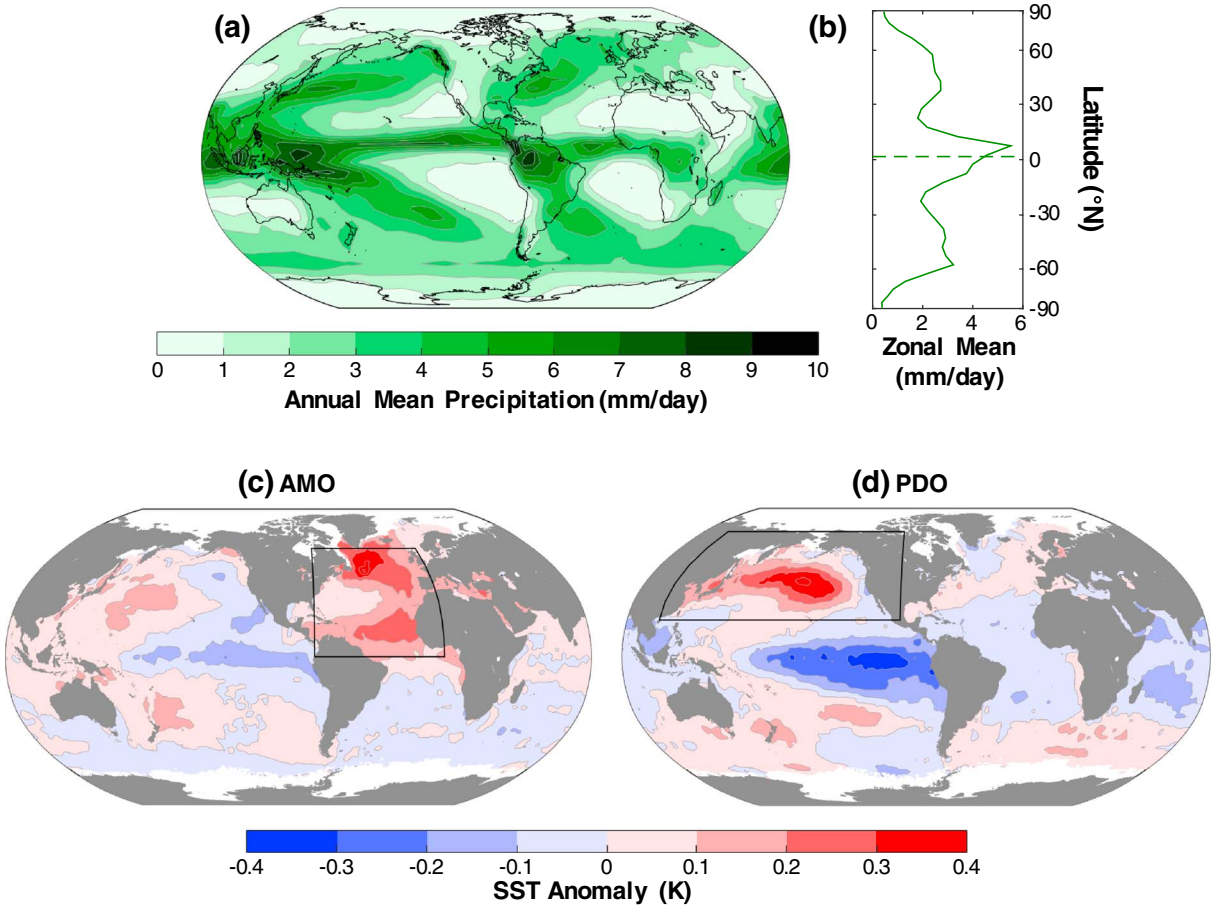

Figure 1. (a) Annual mean precipitation rate (contour interval: 1 mm/d) and its (b) zonal average from the S12 reconstruction. The green dashed line indicates the time mean ITCZ position of 1.7°N. Sea Surface Temperature anomalies regressed against +1σ of the annual mean (c) AMO and (d) PDO indices. The contour interval is 0.1 K. Black lines indicate the regions SSTs are averaged over to generate the AMO and PDO indices.

approach, guided by the energetic framework, to SST-ITCZ-atmospheric circulation relationships established in models but less rigorously studied in observations. For consistency with the *Kang et al.* [2009] framework, we study extratropical SST variability, focusing on multidecadal timescales, and discuss connections between that SST variability and the ocean circulation's energy transport in section 4.

2. Twentieth Century Reconstructions and Reanalyses of SST, Precipitation, and Atmospheric Circulation

Two leading patterns of extratropical NH SST variability are the Atlantic Multidecadal Oscillation (AMO) [*Kerr*, 2000] (Figure 1c) and the Pacific Decadal Oscillation (PDO) [*Mantua et al.*, 1997] (Figure 1d). Using the HadISST version 1.1 reconstruction from 1870 to 2012 [*Rayner et al.*, 2003], we define the AMO index as the difference between average North Atlantic and global mean SST, following *Trenberth and Shea* [2006]. Its time series (Figure 2a) shows variability across a range of timescales, with multiple warm (1924–1966 and 1995–2012) and cold (1902–1923 and 1967–1994) periods lasting several decades. This broad-spectrum variability makes referring to the AMO as an "oscillation" somewhat problematic; however, in keeping with convention, we retain the original acronym. The SST anomalies associated with a 1σ warm anomaly of the annual mean AMO index (+0.14 K) show basin-wide warming in the North Atlantic, peaking at +0.5 K off of the eastern Canadian coast (Figure 1c).

The PDO index is often defined as the first principal component (PC) time series from an empirical orthogonal function (EOF) analysis of monthly mean SST anomalies from 20° to 70°N in the Pacific [*Mantua et al.*, 1997]. When the PC time series is regressed back onto SST, the resulting pattern of SST anomalies shows cooling

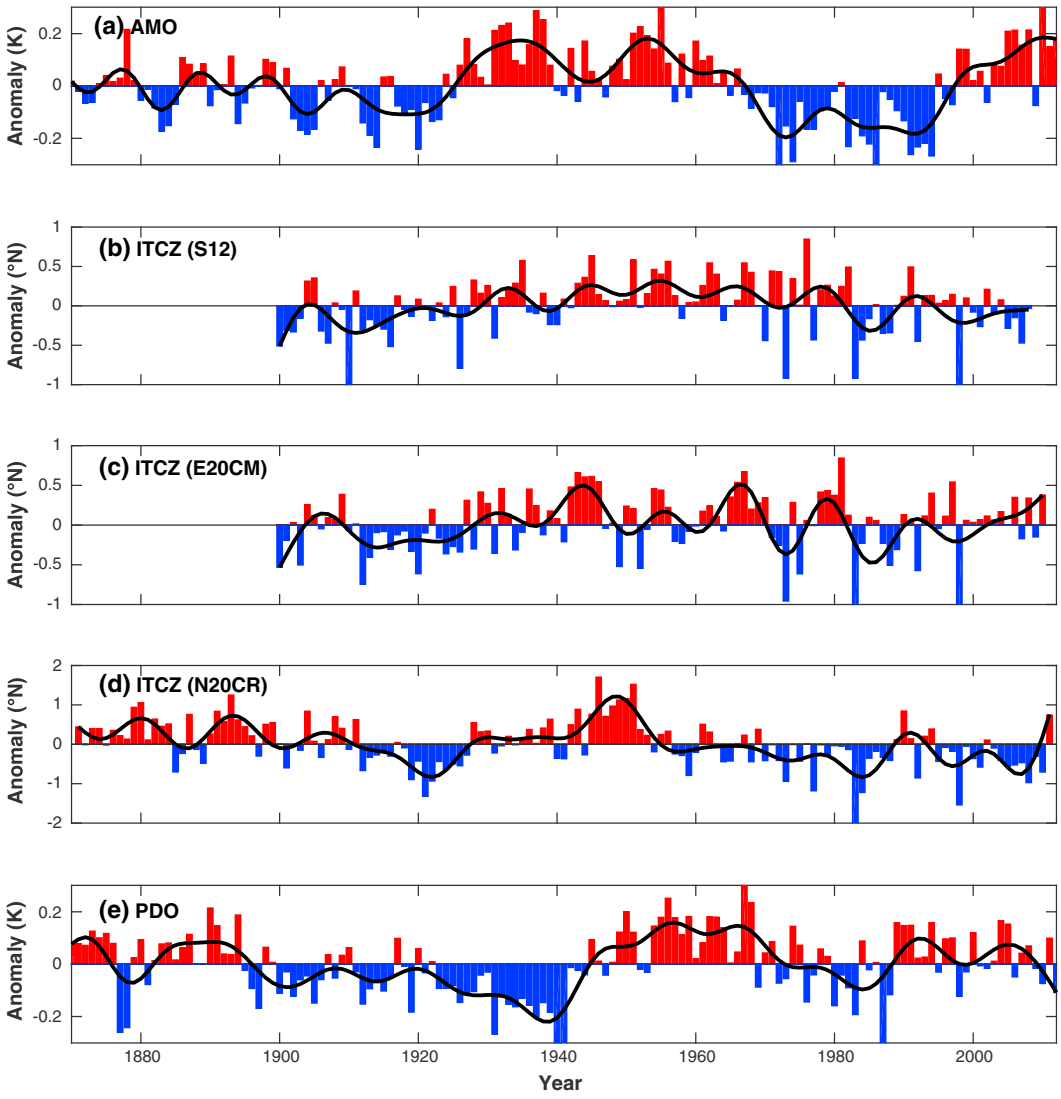

Figure 2. Time series of annual mean (a) AMO index, (b) S12 ITCZ position, (c) E20CM ITCZ position, (d) N20CR ITCZ position, and (e) PDO index anomalies. Black lines indicate time series that have been low-pass-filtered using an order 10 Butterworth filter with a cutoff period of 10 years.

over almost all of the North Pacific [cf. *Deser et al.*, 2010, Figure 10]. Given this pattern of SST anomalies, we simplify the definition of the PDO, calculating its index similarly to the AMO index by removing the global mean SST from its average value between 20°N and 70°N in the Pacific. Our resulting PDO index time series (Figure 2e) and spatial pattern of SST anomalies (Figure 1d) are both highly correlated with those resulting from an EOF analysis as in *Mantua et al.* [1997]; $R = -0.86$ and -0.66, respectively (supporting information Figure S1). Even though it is not identical to the original definition of the PDO, our index is similar enough that we retain the original acronym.

We primarily use the *Smith et al.* [2012, hereafter S12] precipitation reconstruction to analyze precipitation and ITCZ variability. It estimates monthly precipitation rates over the whole globe with a horizontal resolution of 5° and covers the years 1900–2008. Most of the precipitation associated with the ITCZ falls over the ocean, so by estimating precipitation over both land and ocean, S12 provides a better estimate of the ITCZ's position than a land-only reconstruction. Fitting EOFs calculated from the satellite-based Global Precipitation Climatology Project (GPCP) precipitation estimates to the Global Historical Climatology Network (GHCN) rain gauge reconstruction back to 1900, S12 also applies a correction to precipitation over the ocean using available SST and sea level pressure data. Tropical precipitation variability in the S12 reconstruction has been shown to match well with GPCP estimates, and when the reconstruction methodology is applied to an

independent twentieth century reanalysis, it is able to reproduce large-scale multidecadal variability despite its relatively short reference period [*Smith et al.*, 2013]. Estimates of the time mean and zonal mean precipitation climatology are shown in Figures 1a and 1b. The ITCZ is clearly seen in the tropical Atlantic and Pacific, and zonal mean tropical precipitation peaks north of the equator.

Because rain gauge-based precipitation estimates are relatively sparse in the early part of the twentieth century [cf. *Smith et al.*, 2012, Figure 2], we supplement the S12 reconstruction with two atmospheric reanalyses from the National Oceanic and Atmospheric Administration (NOAA) and the European Centre for Medium-Range Weather Forecasts (ECMWF). The NOAA twentieth century reanalysis [*Compo et al.*, 2011] (hereafter N20CR) version 2 has 2° horizontal resolution and covers the years 1871–2011. The ECMWF's twentieth century reanalysis [*Hersbach et al.*, 2015] (hereafter E20CM) covers the years 1900–2010 at 0.125° horizontal resolution. Both reanalyses enforce SST and sea ice concentrations as boundary conditions and are forced by variations in incoming solar radiation, CO_2 concentrations, and aerosols; E20CM is also forced with varying ozone concentrations. Neither reanalysis assimilates observations of humidity, so their resulting precipitation estimates are strongly controlled by each model's treatment of moist physics and are not directly observationally constrained. Consequently, these products are only used in support of the S12 reconstruction.

Defining the position of the ITCZ as the latitude that divides regions of equal total precipitation between 20°N and 20°S (the centroid, following *Donohoe et al.* [2013]), time series of its annual mean anomalies about average positions of 1.7°N, 1.9°N, and 2.1°N for S12, N20CR, and E20CM, respectively, are shown in Figures 2b–2d. The shortcomings of using land-only precipitation to estimate the position of the global ITCZ are highlighted by calculating the centroid of zonal mean land-only precipitation using the satellite-based GPCP product: between 1979 and 2008, R^2 is only 0.04 between annual mean anomalies of the land-only and global centroid time series. When low-pass-filtered to isolate their multidecadal variability, shown as black lines in Figure 2, the S12, E20CM, and N20CR ITCZ time series are correlated, with S12 and E20CM being the most similar: from 1900 to 2008, $R = 0.69$ between S12 and E20CM, 0.49 between S12 and N20CR, and 0.41 between E20CM and N20CR. Additionally, all three products' time series are highly correlated with observed interannual ITCZ variability over the satellite era (supporting information Text S2). While the three time series often differ for a given year, a consistent feature of multidecadal ITCZ variability is seen in all three products: the ITCZ was located southward earlier in the century, farther north after 1930, and moved southward again around 1980.

To estimate atmospheric circulation anomalies, we use the National Centers for Environmental Prediction/National Center for Atmospheric Research (NCEP/NCAR) reanalysis [*Kalnay et al.*, 1996] from 1948 to 2012. We define an index of Hadley cell strength at the equator (Ψ_{eq}) as the value of the vertically averaged mass transport stream function at the equator, and an index of the interhemispheric temperature contrast in the troposphere ($T_{interhem}$) as the difference between NH and SH average temperatures between the surface and 300 hPa. See supporting information Text S1 for additional details on the indices. While the atmospheric circulation and temperatures in the NCEP/NCAR reanalysis are constrained by radiosonde observations, E20CM and N20CR are forced primarily at the surface by SSTs. Tropical SSTs and large-scale precipitation have dynamic and thermodynamic connections (see the review in *Sobel* [2007]), making E20CM and N20CR output useful for studying ITCZ dynamics, but SSTs alone do not sufficiently constrain the atmospheric circulation above the surface. As such, we limit discussions of circulation anomalies in E20CM and N20CR to supporting information Text S3.

3. ITCZ, AMO/PDO, and Tropospheric Covariability on Multidecadal Timescales

To test for connections between extratropical SSTs and the ITCZ position, we perform a multiple regression analysis on the ITCZ position using the AMO and PDO indices as predictors, low-pass filtering each time series using a cutoff period of 10 years to isolate its multidecadal variability (the black lines in Figure 2; see supporting information Text S1 for more details on the regressions). We find that the S12 ITCZ shifts north when the North Atlantic and Pacific are warm: a $+1\sigma$ (+0.14 K) AMO anomaly is associated with a northward ITCZ shift of 0.07° ± 0.05° and a $+1\sigma$ (+0.12 K) PDO anomaly is associated with a northward ITCZ shift of 0.10° ± 0.06°. Error estimates are for a $\pm1\sigma$ confidence interval. The AMO and PDO indices each explain roughly 10% of the ITCZ variance on multidecadal timescales ($R^2 = 0.11$ and 0.14, respectively).

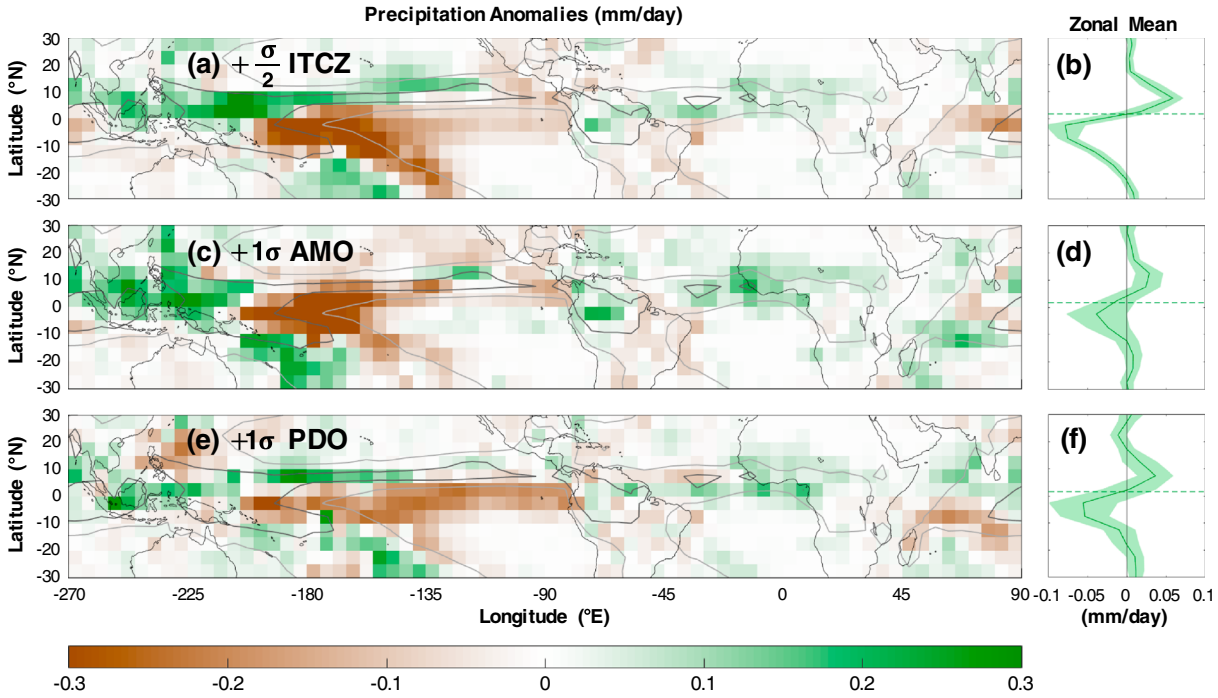

Figure 3. Local precipitation anomalies and their zonal averages regressed against (a, b) $+\sigma/2$ ITCZ shift, (c, d) $+1\sigma$ AMO index, and (e, f) $+1\sigma$ PDO index anomalies. Light and dark grey contours show the 3 mm/d and 6 mm/d climatology of annual mean precipitation, respectively. Green shading around the zonal mean anomalies are $\pm1\sigma$ error estimates, and the green dashed line indicates the time mean ITCZ position.

In the NOAA and ECMWF reanalyses, the ITCZ position is correlated with the AMO index, but not necessarily with the PDO index. The AMO-ITCZ correlations are significant to 1σ (N20CR: $R^2 = 0.12$; E20CM: $R^2 = 0.20$), but the PDO-ITCZ correlations are only significant in the N20CR product ($R^2 = 0.06$). The ITCZ shifts associated with a warm phase AMO are larger in the reanalyses than in S12 but are still within error estimates of each other (supporting information Table S1). It should be noted that the low-pass-filtered AMO and PDO time series are uncorrelated ($R^2 = 0.00$), making the total fraction of the ITCZ's variance explained by the multiple regression analysis equal to the sum of the two R^2 values.

Complex spatial patterns are seen in the precipitation anomalies associated with a northward ITCZ shift (Figure 3a). When low-pass-filtered precipitation anomalies are regressed against a northward shift of the ITCZ position, statistically significant (to 1σ) anomalies in the tropics peak in the West Pacific, with a smaller north-south dipole in the Atlantic. Locally, these anomalies can reflect a pure shift in the ITCZ position (such as those seen in the central Pacific), a contraction/intensification of the local ITCZ (West Pacific), or a combination of the two (Atlantic). In the zonal mean, these anomalies project neatly onto a positive-negative dipole centered on the time mean ITCZ position (Figure 3b), reflecting a northward shift of the precipitation centroid.

Precipitation anomaly patterns indicative of northward ITCZ shifts are also seen when low-pass-filtered anomalies are multiple regressed against the AMO and PDO indices. Maps of S12 precipitation anomalies associated with warm phase AMO and PDO indices (Figures 3c and 3e) have significant (to 1σ) spatial correlations with those associated with a northward ITCZ shift: between 20°N and 20°S, $R_{AMO,ITCZ} = 0.65$ and $R_{PDO,ITCZ} = 0.54$. Statistically significant precipitation anomalies associated with a warm phase AMO show a tripole pattern in the western Pacific similar to those associated with a northward ITCZ shift, and significant positive anomalies in the northern tropical Atlantic and Sahel are consistent with those in *Zhang and Delworth* [2006]. The pattern of anomalies associated with a warm phase PDO is slightly different, with a north-south dipole in the central Pacific. These central Pacific anomalies are statistically significant, but the anomalies in the western and southern Pacific are not. North-south dipoles of precipitation anomalies centered on the time mean ITCZ position are seen when zonal mean precipitation anomalies are multiple-regressed against the AMO and PDO indices (Figures 3d and 3f), consistent with a northward shift of the precipitation centroid.

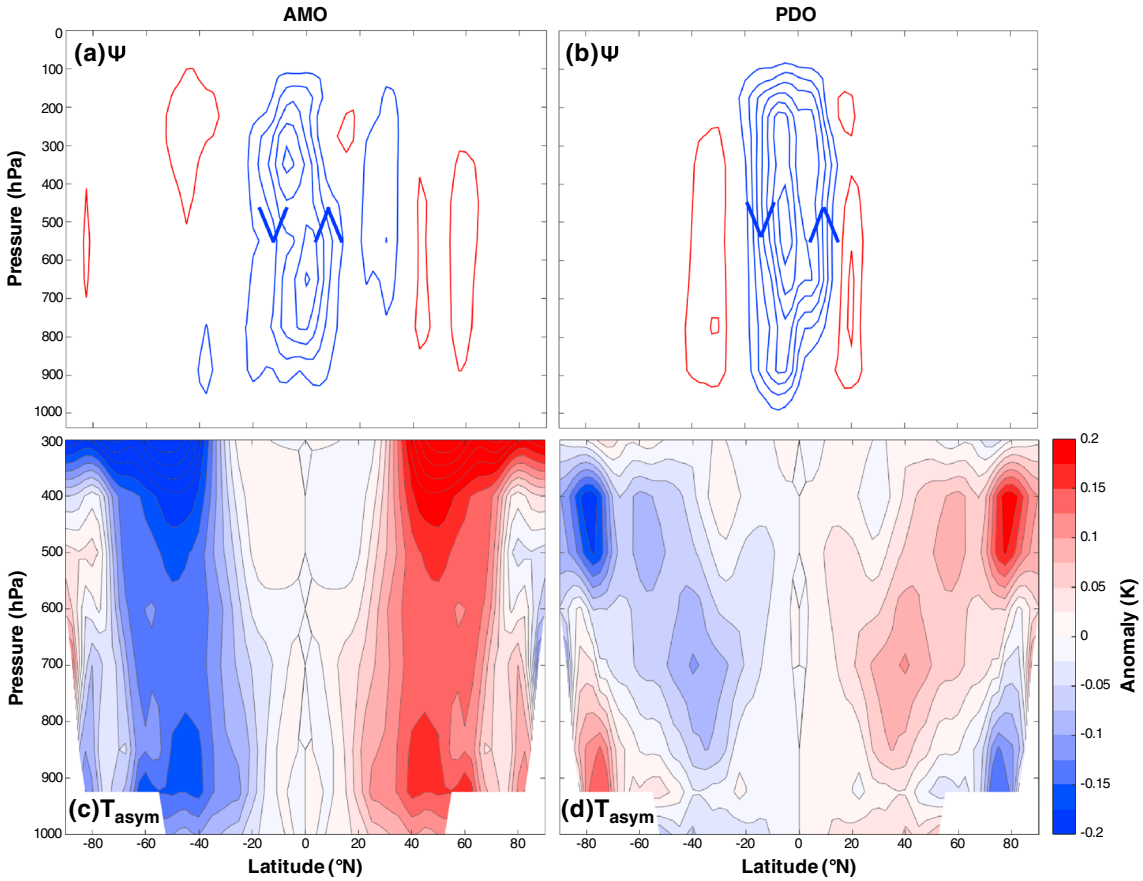

Figure 4. Meridional overturning stream function anomalies from the NCEP/NCAR reanalysis regressed onto (a) $+1\sigma$ AMO and (b) $+1\sigma$ PDO anomalies. Blue contours indicate negative anomalies and counterclockwise rotation, indicated by chevrons, and red contours indicate positive anomalies and clockwise rotation. The contour interval is 1 Sv (10^9 kg/s); the zero contour is not shown. The hemispherically asymmetric component of zonal mean temperature anomalies (see supporting information Text S1) associated with (c) $+1\sigma$ AMO and (d) $+1\sigma$ PDO anomalies. Contour interval: 0.025 K.

In the reanalyses, similar precipitation anomaly patterns are seen for a northward ITCZ shift and a warm North Atlantic, and the anomalies associated with warm phases of the AMO and PDO in both E20CM and N20CR remain largest in the western and central Pacific, respectively (supporting information Figures S2 and S3). The zonal mean precipitation anomalies in supporting information Figure S3f show that the statistically significant PDO-ITCZ position correlation in N20CR is a result of subtropical precipitation anomalies projecting onto the centroid metric, rather than a shift or intensification of the zonal mean tropical precipitation maximum. For the regressions onto both the ITCZ position and local precipitation anomalies, the reanalyses support the AMO-ITCZ connection seen in the S12 reconstruction, but they cast doubt on the connection between the PDO and the ITCZ position.

Consistent with northward ITCZ shifts, we also find correlations between anomalies in the Hadley cells, interhemispheric tropospheric temperature contrasts, and the AMO and PDO indices in the NCEP/NCAR reanalysis. During warm phases of the AMO and PDO, anomalous cross-equatorial Hadley cells are seen (Figures 4a and 4b), with air ascending north of the equator. We also observe anomalous interhemispheric temperature contrasts reflecting a relatively warm NH troposphere (Figures 4c and 4d). Temperature anomalies associated with a warm North Atlantic are spread over the depth of the troposphere with a local maximum near the surface and are significant (to 1σ), while those associated with a warm North Pacific are weaker, peak in the middle troposphere, and are not significant. Conversely, stream function anomalies associated with the PDO are larger than those associated with the AMO. While both sets of stream function anomalies are significant (to 1σ), they are not significantly different from each other.

Regressing the AMO and PDO indices against the Ψ_{eq} and $T_{interhem}$ indices from the NCEP/NCAR reanalysis, we find that the AMO explains more of their variance than the PDO does. At multidecadal timescales, the

AMO index is (to 1σ) significantly correlated with both interhemispheric atmospheric temperature contrasts and cross-equatorial mass transport by the Hadley cells (R^2 = 0.74 and 0.41, respectively). It is remarkable to note that the AMO index explains over 70% of the interhemispheric tropospheric temperature contrast. The somewhat stronger stream function anomalies associated with the PDO in Figure 4b are the result of a regression slope that is larger between the PDO and Ψ_{eq} (27 ± 14 Sverdrup (Sv)/K) than it is between the AMO and Ψ_{eq} (21 ± 7.9 Sv/K). While the PDO is significantly correlated with Ψ_{eq} (R^2 = 0.17), it is not significantly correlated with $T_{interhem}$ (R^2 = 0.02), reflecting the lack of significance in the temperature anomalies in Figure 4d. This suggests different mechanisms connect the AMO and PDO to ITCZ shifts.

4. Discussion of Timescales and Mechanisms

Our observed correlations between a warm North Atlantic, northward ITCZ and Hadley cell shifts, and interhemispheric tropospheric temperature contrasts are all consistent with the framework proposed in *Kang et al*. [2009] in which the atmosphere is forced by an interhemispheric heating contrast. We propose that these correlations are the result of a warm North Atlantic fluxing energy upward into the atmosphere, a cool North Atlantic removing energy from the atmosphere, and that they are at least in part due to variations in the Atlantic Ocean's cross-equatorial energy transport. The relationship between North Atlantic SSTs and surface energy fluxes, though, is a function of timescale. On interannual timescales, warm SSTs are correlated with downward surface energy fluxes, indicating forcing by the atmosphere rather than the ocean [*Gulev et al*., 2013]. The pattern of SST anomalies associated with a high-pass-filtered AMO index (using a 10 year cutoff period) is very similar to that associated with the negative phase of the North Atlantic oscillation (NAO) [*Hurrell*, 1995] (supporting information Figure S4), a measure of internal atmospheric variability [*Marshall et al*., 2001]. The NAO and high-pass-filtered AMO time series are correlated, with $R = -0.34$ between 1870 and 2012, and regressions using a high-pass-filtered AMO index explain much less variance of the ITCZ position (R^2 = 0.04), Ψ_{eq} (R^2 = 0.01), and $T_{interhem}$ (R^2 = 0.24) than the low-pass-filtered time series does. Therefore, we do not expect the *Kang et al*. [2009] framework to apply to interannual AMO-ITCZ variability.

Conversely, on multidecadal timescales a warm North Atlantic is correlated with upward surface energy fluxes [*Gulev et al*., 2013], which we interpret as the ocean circulation forcing the atmosphere by converging heat into the North Atlantic. Stochastic forcing by the atmosphere has been invoked to explain multidecadal SST variability in the North Atlantic [*Clement et al*., 2015, 2016], and after 1990 the AMO sharply transitions from a cool phase to a warm phase without any apparent northward shift of the ITCZ (Figure 2). It is possible that other forcing agents such as greenhouse gases and aerosols are contributing to these late twentieth century SST anomalies [*Friedman et al*., 2013], obscuring the impact of AMOC variability on the atmosphere's energy balance during that period. However, the observed positive SST upward surface energy flux correlation over the full extent of the twentieth century cannot be explained without a role for ocean energy transport convergence [*Zhang et al*., 2016; *O'Reilly et al*., 2016]. Furthermore, the *Kang et al*. [2009] framework employed here only requires an upward flux of energy at the surface into the atmosphere without specifying the processes responsible for that flux.

The mechanisms connecting North Pacific SSTs to ITCZ shifts and Hadley cell anomalies are likely different than for North Atlantic SSTs and the *Kang et al*. [2009] mechanism. The Pacific Ocean transports less energy across the equator than the Atlantic [*Trenberth and Caron*, 2001], and its energy transport is thought to be dominated by shallow wind-driven circulations rather than a deep overturning circulation like the AMOC [*Ferrari and Ferreira*, 2011]. Decadal SST variability in the North Pacific may be forced by, for example, the El Niño–Southern Oscillation (ENSO), ocean circulation variability, and extratropical atmospheric variability [*Schneider and Cornuelle*, 2005], making PDO-ITCZ connections likely the result of a combination of processes. When the annual mean Niño-3 index leads the ITCZ time series by 1 year, aligning southward ITCZ shifts with major El Niño events in 1982, 1991, and 1997, we find significant correlations between the two. For the S12, E20CM, and N20CR products, R^2 between the two time series is 0.25, 0.15, and 0.19, respectively. We also find significant correlations at the same 1 year lead between the Niño-3 index and the annual mean Ψ_{eq} index in the NCEP/NCAR reanalysis (R^2 = 0.17), but not with the $T_{interhem}$ index (R^2 = 0.00). *Schneider et al*. [2014] argue that heating of the tropical atmosphere at the equator during an El Niño event alters the energy balance there and shifts the ITCZ toward the equator, with the ITCZ shifting farther from the equator during a

La Niña event. Even though tropical Pacific SSTs do not have much power beyond interannual timescales [cf. *Deser et al*., 2010, Figure 5], their apparent ability to affect both the PDO and ITCZ shifts hint at their potential impact on PDO-ITCZ connections on multidecadal timescales.

In conclusion, we have shown that the AMO explains a significant fraction of multidecadal ITCZ variance across several estimates of twentieth century precipitation, but those estimates disagree on the influence of the PDO. In particular, the AMO explains 41% of Hadley cell variability at the equator and a remarkable 74% of interhemispheric tropospheric temperature variability in the NCEP/NCAR reanalysis. Our results suggest that heating and cooling of the extratropical atmosphere, as proposed in *Kang et al*. [2009], connect the ITCZ position to the AMO; the mechanisms connecting the ITCZ position to the PDO are less clear. It is believed that on multidecadal timescales the AMO is affected by variations in the strength of the AMOC (see the review by *Buckley and Marshall* [2016]), a driver of climate and climate variability that connects the two hemispheres. Moreover, the AMOC has predictability on decadal timescales [*Tulloch and Marshall*, 2012], suggesting that AMOC predictability could be leveraged for the predictability of ITCZ migrations, with implications for precipitation variability along the entire tropical belt.

Acknowledgments

This study was supported by a grant from NOAA. The S12 reconstruction is available at http://cics.umd.edu/~tsmith/recpr/eof1/full/. The HadISST product is available at http://www.metoffice.gov.uk/hadobs/hadisst/. The E20CM reanalysis is available at http://www.ecmwf.int/en/research/climate-reanalysis/era-20cm-model-integrations. The N20CR reanalysis is available at http://www.esrl.noaa.gov/psd/data/gridded/data.20thC_ReanV2.html. The NCEP/NCAR reanalysis is available at http://www.esrl.noaa.gov/psd/data/gridded/data.ncep.reanalysis.html. The authors thank three anonymous reviewers for their insightful comments.

References

Adler, R. F., et al. (2003), The version-2 Global Precipitation Climatology Project (GPCP) monthly precipitation analysis (1979–present), *J. Hydrometeorol.*, *4*, 1147–1167, doi:10.1175/1525-7541(2003)004<1147:TVGPCP>2.0.CO;2.

Bretherton, C. S., M. Widmann, V. P. Dymnikov, J. M. Wallace, and I. Blade (1999), The effective number of spatial degrees of freedom of a time-varying field, *J. Clim.*, *12*(7), 1990–2009, doi:10.1175/1520-0442(1999)012<1990:TENOSD>2.0.CO;2.

Broccoli, A. J., K. A. Dahl, and R. J. Stouffer (2006), Response of the ITCZ to Northern Hemisphere cooling, *Geophys. Res. Lett.*, *33*, L01702, doi:10.1029/2005GL024546.

Buckley, M., and J. Marshall (2016), Observations, inferences, and mechanisms of the Atlantic Meridional Overturning Circulation: A review, *Rev. Geophys.*, *54*, 5–63, doi:10.1002/2015RG000493.

Chiang, J. C. H., and C. M. Bitz (2005), Influence of high latitude ice cover on the marine Intertropical Convergence Zone, *Clim. Dyn.*, *25*(5), 477–496, doi:10.1007/s00382-005-0040-5.

Chiang, J. C. H., and A. R. Friedman (2012), Extratropical cooling, interhemispheric thermal gradients, and tropical climate change, *Annu. Rev. Earth Planet. Sci.*, *40*(1), 383–412, doi:10.1146/annurev-earth-042711-105545.

Clement, A., K. Bellomo, L. N. Murphy, M. A. Cane, T. Mauritsen, G. Radel, and B. Stevens (2015), The Atlantic Multidecadal Oscillation without a role for ocean circulation, *Science*, *350*(6258), 320–324, doi:10.1126/science.aab3980.

Clement, A., M. A. Cane, L. N. Murphy, K. Bellomo, T. Mauritsen, and B. Stevens (2016), Response to comment on "The Atlantic Multidecadal Oscillation without a role for ocean circulation", *Science*, *352*(6293), 1527–1527, doi:10.1126/science.aaf2575.

Compo, G. P., et al. (2011), The twentieth century reanalysis project, *Q. J. R. Meteorol. Soc.*, *137*(654), 1–28, doi:10.1002/qj.776.

Deser, C., M. A. Alexander, S.-P. Xie, and A. S. Philips (2010), Sea surface temperature variability: Patterns and mechanisms, *Annu. Rev. Mar. Sci.*, *2*, 115–143, doi:10.1146/annurev-marine-120408-151453.

Donohoe, A., J. Marshall, D. Ferreira, and D. McGee (2013), The relationship between ITCZ location and cross-equatorial atmospheric heat transport: From the seasonal cycle to the Last Glacial Maximum, *J. Clim.*, *26*(11), 3597–3618, doi:10.1175/JCLI-D-12-00467.1.

Donohoe, A., J. Marshall, D. Ferreira, K. Armour, and D. McGee (2014), The interannual variability of tropical precipitation and interhemispheric energy transport, *J. Clim.*, *27*(9), 3377–3392, doi:10.1175/JCLI-D-13-00499.1.

Ferrari, R., and D. Ferreira (2011), What processes drive the ocean heat transport?, *Ocean Model.*, *38*(3), 171–186, doi:10.1016/j.ocemod.2011.02.013.

Friedman, A. R., Y.-T. Hwang, J. C. Chiang, and D. M. W. Frierson (2013), Interhemispheric temperature asymmetry over the twentieth century and in future projections, *J. Clim.*, *26*(15), 5419–5433, doi:10.1175/JCLI-D-12-00525.1.

Frierson, D. M. W., and Y.-T. Hwang (2012), Extratropical influence on ITCZ shifts in slab ocean simulations of global warming, *J. Clim.*, *25*(2), 720–733, doi:10.1175/JCLI-D-11-00116.1.

Frierson, D. M. W., Y.-T. Hwang, N. S. Fuckar, R. Seager, S. M. Kang, A. Donohoe, E. A. Maroon, X. Liu, and D. S. Battisti (2013), Contribution of ocean overturning circulation to tropical rainfall peak in the Northern Hemisphere, *Nat. Geosci.*, *6*(11), 940–944, doi:10.1038/ngeo1987.

Gulev, S. K., M. Latif, N. Keenlyside, W. Park, and K. Koltermann (2013), North Atlantic Ocean control on surface heat flux on multidecadal timescales, *Nature*, *499*(7459), 464–467, doi:10.1038/nature12268.

Hersbach, H., C. Peubey, A. Simmons, P. Berrisford, P. Poli, and D. Dee (2015), ERA-20CM: A twentieth-century atmospheric model ensemble, *Q. J. R. Meteorol. Soc.*, *141*(691), 2350–2375, doi:10.1002/qj.2528.

Hurrell, J. W. (1995), Decadal trends in the North Atlantic Oscillation: Regional temperatures and precipitation, *Science*, *269*(5224), 676–679, doi:10.1126/science.269.5224.676.

Kalnay, E., et al. (1996), The NCEP/NCAR 40-year reanalysis project, *Bull. Am. Meteorol. Soc.*, *77*(3), 437–471, doi:10.1175/1520-0477(1996)077<0437:TNYRP>2.0.CO;2.

Kang, S. M., D. M. W. Frierson, and I. M. Held (2009), The tropical response to extratropical thermal forcing in an idealized GCM: The importance of radiative feedbacks and convective parameterization, *J. Atmos. Sci.*, *66*(9), 2812–2827, doi:10.1175/2009JAS2924.1.

Kerr, R. A. (2000), A North Atlantic climate pacemaker for the centuries, *Science*, *288*(5473), 1984–1985, doi:10.1126/science.288.5473.1984.

Mantua, N. J., S. R. Hare, Y. Zhang, J. M. Wallace, and R. C. Francis (1997), A Pacific interdecadal climate oscillation with impacts on salmon production, *Bull. Am. Meteorol. Soc.*, *78*(6), 1069–1079, doi:10.1175/1520-0477(1997)078<1069:APICOW>2.0.CO;2.

Marshall, J., Y. Kushnir, D. Battisti, P. Chang, A. Czaja, R. Dickson, J. Hurrell, M. McCartney, R. Saravanan, and M. Visbeck (2001), North Atlantic climate variability: Phenomena, impacts and mechanisms, *Int. J. Climatol.*, *21*(15), 1863–1898, doi:10.1002/joc.693.

Marshall, J., A. Donohoe, D. Ferreira, and D. McGee (2014), The ocean's role in setting the mean position of the Inter-Tropical Convergence Zone, *Clim. Dyn.*, *42*, 1967–1979, doi:10.1007/s00382-013-1767-z.

McGee, D., A. Donohoe, J. Marshall, and D. Ferreira (2014), Changes in ITCZ location and cross-equatorial heat transport at the Last Glacial Maximum, Heinrich Stadial 1, and the mid-Holocene, *Earth Planet. Sci. Lett.*, *390*, 69–79, doi:10.1016/j.epsl.2013.12.043.

O'Reilly, C. H., M. Huber, T. Woollings, and L. Zanna (2016), The signature of low frequency oceanic forcing in the Atlantic Multidecadal Oscillation, *Geophys. Res. Lett.*, *43*, 2810–2818, doi:10.1002/2016GL067925.

Rayner, N. A., D. E. Parker, E. B. Horton, C. K. Folland, L. V. Alexander, D. P. Rowell, E. C. Kent, and A. Kaplan (2003), Global analyses of sea surface temperature, sea ice, and night marine air temperature since the late nineteenth century, *J. Geophys. Res.*, *108*(D14), 4407, doi:10.1029/2002JD002670.

Schneider, N., and B. D. Cornuelle (2005), The forcing of the Pacific Decadal Oscillation*, *J. Clim.*, *18*(21), 4355–4373, doi:10.1175/JCLI3527.1.

Schneider, T., T. Bischoff, and G. H. Haug (2014), Migrations and dynamics of the intertropical convergence zone, *Nature*, *513*, 45–53, doi:10.1038/nature13636.

Smith, T. M., P. A. Arkin, L. Ren, and S. S. P. Shen (2012), Improved reconstruction of global precipitation since 1900, *J. Atmos. Oceanic Technol.*, *29*(10), 1505–1517, doi:10.1175/JTECH-D-12-00001.1.

Smith, T. M., S. S. P. Shen, L. Ren, and P. A. Arkin (2013), Estimating monthly precipitation reconstruction uncertainty beginning in 1900, *J. Atmos. Oceanic Technol.*, *30*(6), 1107–1122, doi:10.1175/JTECH-D-12-00197.1.

Sobel, A. H. (2007), Simple models of ensemble-averaged precipitation and surface wind, given the sea surface temperature, in *The Global Circulation of the Atmosphere*, edited by T. Schneider and A. H. Sobel, pp. 219–251, Princeton Univ. Press, Princeton, N. J.

Sun, C., J. Li, F.-F. Jin, and R. Ding (2013), Sea surface temperature inter-hemispheric dipole and its relation to tropical precipitation, *Environ. Res. Lett.*, *8*(4), doi:10.1088/1748-9326/8/4/044006.

Trenberth, K. E., and J. M. Caron (2001), Estimates of meridional atmosphere and ocean heat transports, *J. Clim.*, *14*(16), 3433–3443, doi:10.1175/1520-0442(2001)014<3433:EOMAAO>2.0.CO;2.

Trenberth, K. E., and D. J. Shea (2006), Atlantic hurricanes and natural variability in 2005, *Geophys. Res. Lett.*, *33*, L12704, doi:10.1029/2006GL026894.

Tulloch, R., and J. Marshall (2012), Exploring mechanisms of variability and predictability of Atlantic meridional overturning circulation in two coupled climate models, *J. Clim.*, *25*(12), 4067–4080, doi:10.1175/JCLI-D-11-00460.1.

Zhang, R., and T. L. Delworth (2005), Simulated tropical response to a substantial weakening of the Atlantic thermohaline circulation, *J. Clim.*, *18*(12), 1853–1860, doi:10.1175/JCLI3460.1.

Zhang, R., and T. L. Delworth (2006), Impact of Atlantic multidecadal oscillations on India/Sahel rainfall and Atlantic hurricanes, *Geophys. Res. Lett.*, *33*, L17712, doi:10.1029/2006GL026267.

Zhang, R., T. L. Delworth, and I. M. Held (2007), Can the Atlantic Ocean drive the observed multidecadal variability in Northern Hemisphere mean temperature?, *Geophys. Res. Lett.*, *34*, L02709, doi:10.1029/2006GL028683.

Zhang, R., R. Sutton, G. Danabasoglu, T. L. Delworth, W. M. Kim, J. Robson, and S. G. Yeager (2016), Comment on "The Atlantic Multidecadal Oscillation without a role for ocean circulation", *Science*, *352*(6293), 1527–1527, doi:10.1126/science.aaf1660.